

Computational Study of Antagonist/ α_{1A} Adrenoceptor Complexes—Observations of Conformational Variations on the Formation of Ligand/Receptor Complexes

Gemma K. Kinsella,[†] Isabel Rozas,^{*,†,‡} and Graeme W. Watson^{*,†}

School of Chemistry and Centre for Synthesis and Chemical Biology, University of Dublin, Trinity College, Dublin 2, Ireland

Received April 21, 2005

As selective antagonist inhibition may relieve the symptoms of benign prostatic hyperplasia, we have examined the interactions of antagonists including quinazoline and imidazolidinium/guanidinium compounds complexed with a homology model of the α_{1A} adrenoceptor. Our approach involves docking of ligands of various structural classes followed by molecular dynamics simulations of antagonist/receptor complexes, which demonstrates that different structural classes of antagonist induce different receptor conformations upon binding with particular variations noted in the conformation of TM-V. Subsequently, we examined the interactions and the conformational flexibility of α_1 and α_{1A} adrenoceptor antagonists, with the ligand-induced receptor conformers. This study indicated that a receptor conformation induced by one structural class of antagonist is not suitable for direct screening of another class. Our analysis indicates that computational high-throughput screening is likely to give inaccurate data on binding and selectivity and such studies need to consider conformational changes in the receptor.

Introduction

The broad spectrum of signals transduced by G protein coupled receptors (GPCRs) makes them one of the most intriguing pharmacological targets, with approximately 52% of all existing drugs acting on GPCRs.¹ The α_1 adrenoceptor (α_1 -AR) family, which belongs to class A of GPCRs, is of particular therapeutic interest due to their important role in control of blood pressure and the contraction and growth of smooth muscle. More specifically, the α_{1A} -AR subtype, located in large abundance in the prostate, is thought to be influential in the condition known as benign prostatic hyperplasia (BPH).² BPH affects as many as 60% of men over the age of 60 and the number of patients is rising worldwide as a result of the aging population.³

α -AR blockers relax smooth muscles and are prescribed to approximately 80% of patients being treated for BPH.⁴ In this work, we examine a number of such antagonists currently used, including prazosin, terazosin, doxazosin, and alfuzosin (see Figure 1 for structures and Table 1 for activities).⁵ These quinazoline-based antagonists were originally developed as antihypertensives and their ameliorative effects in the treatment of BPH were not observed until their introduction into clinical practice. Ongoing research increasingly suggests that use of selective α_{1A} -AR antagonists, such as tamsulosin, may offer an advantage over nonselective α_1 -AR blockers, as they allow administration of therapeutic doses with fewer side effects.⁶ Two families of compounds with 2-iminoimidazolidinium and bis-guanidinium cations at both ends of a linker formed by diphenyl derivatives were found to exhibit α_{1A} -AR antagonist activity (1–8, Figure 1).⁷ Pharmacological studies on slices of human prostate with BPH showed that the guanidinium derivatives were able to inhibit between 90 and 95% of the contractions induced by noradrenaline.⁸ These results are comparable to the 95% inhibition observed for the clinically used antagonist doxazosin.⁸

A further literature review of α_1 -AR antagonists in the treatment of BPH yielded, among others, the piperazine pyri-

midinedione derivatives 5-methylurapidyl (9)⁹ and RS-100,975 (10),¹⁰ which are antagonists of the $\alpha_{1A/1D}$ -ARs, and the piperazine oxazoline derivative RWJ-37914 (11), which exhibited very good selectivity toward the α_{1A} -AR.¹¹ A number of benzodioxanes were also prepared and tested by Barbaro et al.,¹² such as compound 12, while Chern et al.¹¹ prepared α_1 -AR antagonists that included tricyclic fused quinazolines of which compound 13 exhibited the largest α_{1A} -AR selectivity over α_{1B} -AR (Figure 2).

A variety of α_{1A} -AR antagonists contain a single nitrogen in an alkyl chain, including the benzodioxan derivatives related to WB-4101 (14), a known α_1 -AR antagonist. Quaglia et al.¹⁴ included a phenyl ring and developed phendioxan (15) with a marked drop in affinity toward the α_{1B} - and α_{1D} -AR subtypes, while not affecting the affinity for the α_{1A} -AR subtype. Further work resulted in the development of compound 16 as a potent and selective antagonist for the α_{1A} -AR. In addition, RS-17053 (17) is an α_{1A} -AR subtype-selective antagonist, which displays 126- and 50-fold selectivity over human α_{1B} - and α_{1D} -ARs, respectively (Figure 2 and Table 1).¹⁵

The development of high-affinity α_{1A} -AR antagonists is of paramount importance for the treatment of BPH. However, a detailed understanding of their binding interactions has been hampered due to the unknown three-dimensional conformation of the α_{1A} -AR. At present, the most thoroughly documented example of a membrane protein is rhodopsin, which was first crystallized in its inactive state in 2000 and has been subsequently used for many homology modeling studies of class A GPCRs.¹⁶ The rhodopsin conformation, consisting of a bundle of seven transmembrane α helices (TMI–VII), was further refined to a resolution of 2.6 Å in 2002 (PDB ID 1I9h),¹⁷ which was used in our previous homology modeling study.¹⁸

Bissantz et al.¹⁹ developed similar rhodopsin-derived GPCR models of the dopamine D₃, muscarinic M₁, and vasopressin V_{1a} receptors, which were used for direct rigid docking of antagonists. Recently, Evers et al.²⁰ developed an α_{1A} -AR model utilizing a docked antagonist as an additional restraint in the modeling procedure. They subsequently performed virtual screening of a library of ligands and concluded that rhodopsin-

* To whom correspondence should be addressed. Phone: +353 1 608 3731/1357. Fax: +353 1 671 2826. E-mail: I.R., rozasi@tcd.ie; G.W.W., watson@tcd.ie.

[†] School of Chemistry.

[‡] Centre for Synthesis and Chemical Biology.

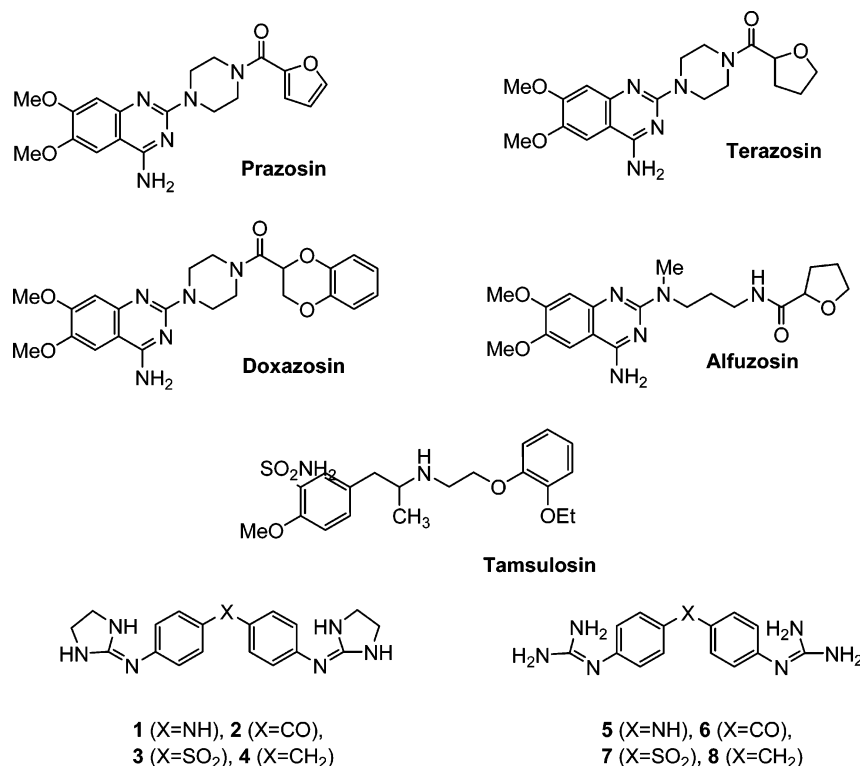


Figure 1. α_1 - and α_{1A} -AR antagonists used clinically (doxazosin, prazosin, terazosin, alfuzosin, and tamsulosin) and the antagonists previously prepared by us (**1–8**).⁷ The protonated nitrogens include the 1-nitrogen position of the quinazolinone ring for the current clinical antagonists and the connecting nitrogens of the 2-iminoimidazolidinium and bis-guanidinium compounds.

Table 1. Antagonists and Their Activities Taken from the Study of Bremner et al.⁵ and References Therein

| compd | | activity K_I (nM) | | |
|-----------|------------------|---------------------|---------------|---------------|
| no. | name | α_{1A} | α_{1B} | α_{1C} |
| | prazosin | 0.2 | 0.25 | 0.32 |
| | terazosin | 6.3 | 2.0 | 2.5 |
| | doxazosin | 3.16 | 1.0 | 4.0 |
| | alfuzosin | 10 | 10 | 3.16 |
| 9 | 5-methylurapidil | 0.63 | 40 | 10 |
| 10 | RS-100975 | 1.0 | 79 | 100 |
| 14 | WB4101 | 0.16 | 2.5 | 0.25 |
| 17 | RS-17053 | 0.6 | 16 | 16 |

based homology models may be used as the structural basis for GPCR lead finding and compound optimization. Similarly, we believe that the inactive crystal conformation template is not directly suitable for docking purposes, as the modeled binding sites are often too narrow to accommodate large antagonists. The study of Evers et al. addressed this point through additional restraints in the modeling procedure. However, as the function of a receptor is the result of a conformational change induced by the recognition process toward the ligand, through our molecular modeling studies we aim to facilitate the integration of the available experimental observations and biophysical data into a scheme to examine receptor conformation and functional blockade. Thus, we have developed a computational strategy to produce ligand induced receptor conformations, which could be utilized in further docking and molecular dynamics (MD) simulations with subsequent examination of ligand interactions and binding modes.

Results

Docking and Molecular Dynamics Simulations of Antagonist/ α_{1A} -AR Complexes. Upon statically docking and then optimizing doxazosin with the α_{1A} -AR model, the 4-amino and

the 6-methoxy groups of the drug form ionic interactions with Asp106 ($d[N\cdots O] = 2.88 \text{ \AA}/d[C\cdots O] = 2.50 \text{ \AA}$), while the 7-methoxy group is close to Ser188 ($d[C\cdots O] = 4.28 \text{ \AA}$). The EC-II residues are in close proximity to the binding site, allowing for interactions with Gln177, as also observed by Pedretti et al.²¹ Over the course of the MD simulation (1 ns), a long lasting ionic interaction was maintained between the protonated nitrogen and Asp106, while there were sporadic contacts of the neighboring methoxy group also with Asp106.

For the tamsulosin complex, a different orientation of the ligand within the binding pocket was determined, with no initial contact being formed with Asp106. The protonated amine moiety is closer to Ser188 ($d[N\cdots O] = 3.90 \text{ \AA}$), while the sulfonamide is close to residues 177–179 of EC-II. Upon monitoring the percentage of ionic interaction occurrence over the MD simulation (1 ns), it is evident that dynamics are essential to allow for reorientation of the molecules and optimization of the ionic interactions. Indeed, the sulfonamide moiety of tamsulosin forms an interaction with Asp106 over the equilibration period, which remains steady throughout the production run. Additionally, the EC-II residues form an interaction with Ile178, which remains largely formed throughout the simulation. There are also interactions involving the protonated nitrogen and the adjacent methyl linker with Glu180.

Finally, when docking compound **6** to the α_{1A} -AR, one guanidinium moiety forms ionic interactions with Asp106 ($d[N\cdots O] = 2.50 \text{ \AA}$) and Ile178 ($d[N\cdots O] = 3.68 \text{ \AA}$). The alternative guanidinium moiety is positioned close to Ser192 of TM-V, while the bridging carbonyl group is close to Ser188. Over the MD simulation (1 ns), one of the connecting nitrogens is near to the carboxylate oxygen of Asp106 steadily throughout the simulation, while the EC-II residues Ile178 and Glu180 interact with one of the outer guanidinium nitrogen groups. At the other guanidinium moiety, there is a steady interaction with

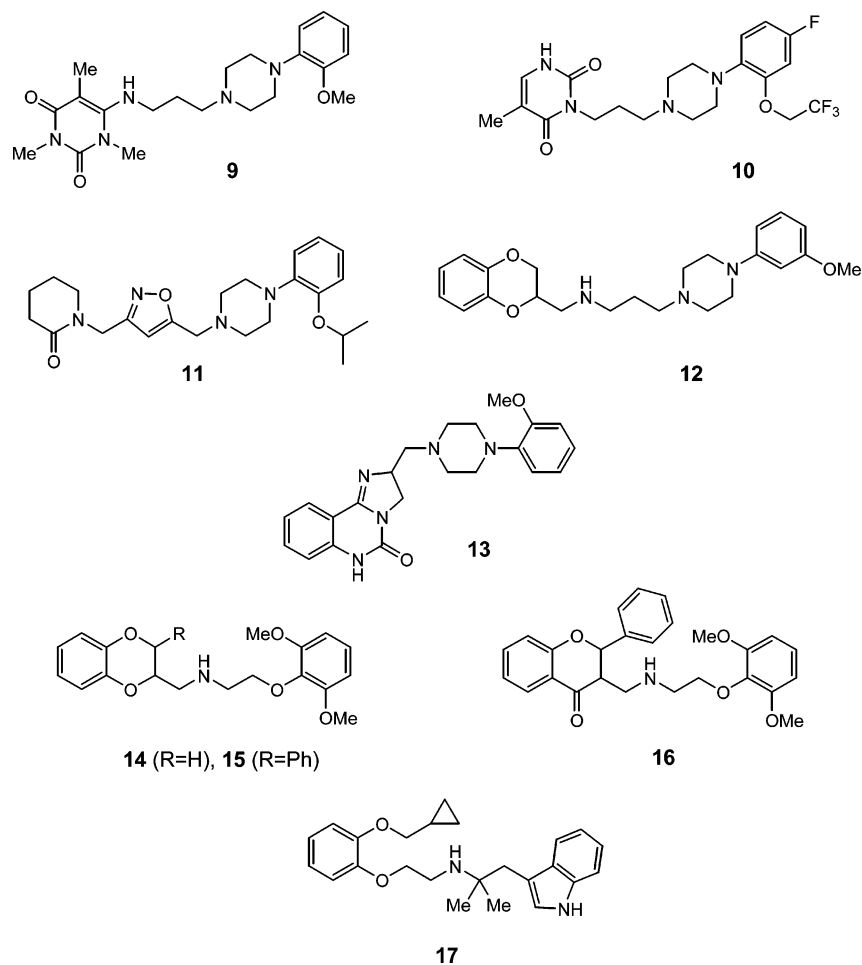


Figure 2. Antagonists of the α_{1A} -AR subtype developed by different authors (9–17). The protonated nitrogens included a nitrogen of the piperazine ring for compounds 9, 10, and 13, a linker nitrogen for compounds 11 and 12, and the sole nitrogen for compounds 14–17.

Ser192 and Trp285. The packing of the transmembrane helices are stabilized by a network of hydrophobic interactions, in which the aromatic residues play a crucial role. For example, Phe193, Tyr194 (TM-V), Trp285, Phe288, Phe289 (TM-VI), Phe308, Phe312, Trp313, and Tyr316 (TM-VII) form an aromatic cluster, in which Trp285 takes a central position.³⁵ In many “rhodopsin-like” GPCRs, ligand binding may occur to a cluster of aromatic residues such as Trp285, Phe288, and Phe289 in TM-VI. Interactions of the ligands with residues in this aromatic cluster are hypothesized to further induce or stabilize an altered configuration of the side chains within this cluster.²²

The structural effects induced on the α_{1A} -AR by the three antagonists doxazosin, tamsulosin, and compound 6 were examined by monitoring the time-dependent helical root-mean-square deviations (rmsd) over the MD simulations. While little structural change occurred during the optimization step, larger changes were observed over the equilibration periods, which stabilized over the production runs. An example of the time-dependent rmsd's is shown for the tamsulosin/ α_{1A} -AR complex simulation (see Figure 3). The most significant structural changes involved TM-II and TM-IV over the heating and equilibration period, which despite a rise in the region of 500–600 ps were largely stabilized over the production period.

Structural Analysis after Molecular Dynamics Simulations of Antagonist/ α_{1A} -AR Complexes. The antagonist/ α_{1A} -AR complexes were averaged over the last 200 ps of the simulations, optimized, and termed α_{1A} -Dox, α_{1A} -Tam, and α_{1A} -6. Determination of the differences between the inactive and “antagonist-bound” forms of the receptor requires comparisons

with an uncomplexed inactive form, which has been equilibrated under the same conditions, such as that developed in our previous study.¹⁸ A large overall rmsd was observed for the C α atoms of the complexes from the uncomplexed conformation in the range of 5.93–6.60 Å (see Table 2). We observe notable rmsd's for TM-III and TM-IV between the uncomplexed receptor conformation and the different complexed conformers after the three simulations (Figure 4).

Furthermore, Pro residues (20 present in the α_{1A} -AR) can have a significant effect in modulating the conformation of TM helices. In the case of the α_{1A} -Dox complex, the largest structural change in the receptor was observed in the region of TM-V around Pro196, which may be important in the movement from the inactive form of the receptor. Ballesteros et al.²³ and Sansom et al.²⁴ examined the role of Pro residues in modulating the conformation of TM helices and suggested that these motifs can function as flexible hinges, inducing a significant bend in the helix, and may play a functional role by supporting alternative helical conformations, which could be used to signal from one side of a bilayer to the other.²⁵ Different conformations at the Pro196 portion of the helix emerge due to flexibility about the Pro residue. The torsional angle between the C α atoms of Leu195/Pro196/Leu197/Ala198 was 47.4° for the uncomplexed receptor, 79.8° for the α_{1A} -Dox conformation, 69.5° for the α_{1A} -Tam conformation, and 58.0° for the α_{1A} -6 conformation.

For the α_{1A} -Dox complex, the methoxy groups of the quinazoline portion of doxazosin are orientated toward the middle of TM-III and Pro196 of TM-V. The benzopyrane moiety is also orientated toward both the extracellular side of

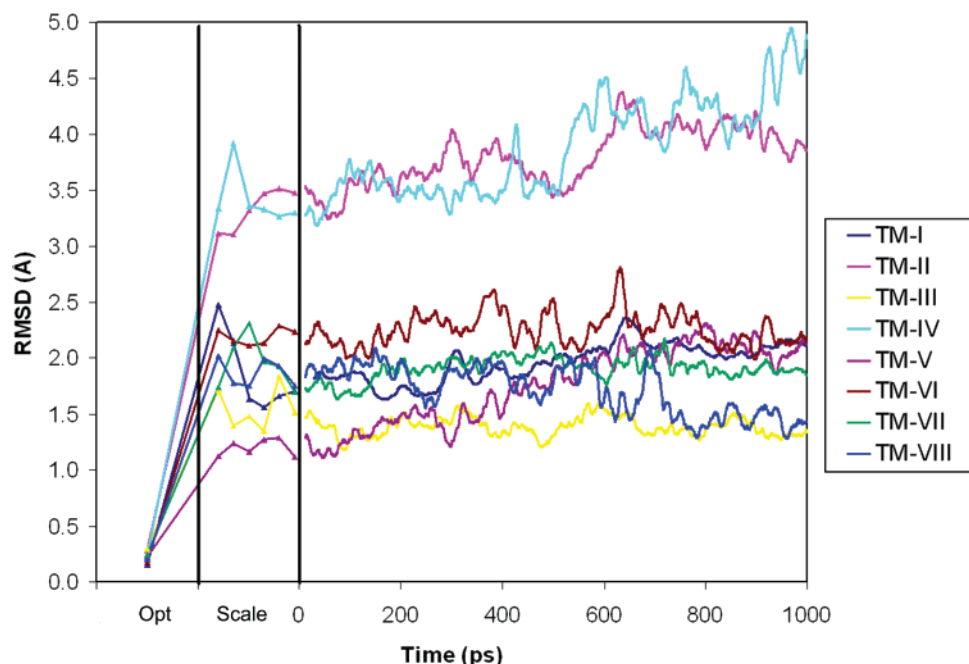


Figure 3. Root mean square deviations in Å for the tamsulosin/ α_{1A} -AR simulation. Optimization and scaling steps, followed by the moving average trend lines (period of 50 ps) over the production run (1 ns).

Table 2. Root Mean Square Deviations in Å for Helices of Selected Antagonist Complexes from the Uncomplexed Receptor, after 1-ns MD Simulations

| | α_{1A} [Dox] | α_{1A} [Tam] | α_{1A} [6] |
|------------------|---------------------|---------------------|-------------------|
| TM-I | 1.42 | 2.55 | 3.30 |
| TM-II | 2.67 | 2.74 | 3.29 |
| TM-III | 2.07 | 1.75 | 1.69 |
| TM-IV | 2.21 | 1.78 | 3.14 |
| TM-V | 2.65 | 2.88 | 2.09 |
| TM-VI | 3.63 | 2.41 | 3.84 |
| TM-VII | 2.06 | 2.51 | 2.66 |
| TM-VIII | 1.01 | 1.86 | 1.78 |
| C α (all) | 6.60 | 5.93 | 6.44 |

TM-V and TM-VI. For the α_{1A} -Tam and α_{1A} -6 complexes, there is a different orientation of the ligand in the binding site compared to that of doxazosin. For the tamsulosin and compound 6 optimized complexes, additional space is created due to movement of Pro196 of TM-V. Furthermore, the antagonists contact with the extracellular end of TM-III and not with the extracellular end of TM-V, which undergoes a marked helical straightening for the tamsulosin complex. Hence, the increased flexibility achieved through the current MD simulations allows for structural optimization of the three final antagonist complexes with respect to the uncomplexed α_{1A} -AR.

Interactions of Structurally Similar Antagonists with the Ligand-Induced α_{1A} -ARs. In the following section, we utilize the developed "antagonist-bound" receptor conformers with the ligands removed, termed α_{1A} [Dox], α_{1A} [Tam], and α_{1A} [6], for redocking antagonists of the same structural class. The receptor conformation α_{1A} [Dox] was utilized for redocking the quinazoline class, the α_{1A} [Tam] receptor conformation for redocking tamsulosin, and receptor conformation α_{1A} [6] for redocking the bis-guanidinium and bis-2-imino-imidazolidinium compounds (1–8). MD simulations (500 ps) were performed to examine the different binding modes of the antagonists.

For interactions of the quinazoline antagonists with receptor conformation α_{1A} [Dox], only doxazosin forms an ionic interaction between the 4-amino group and Asp106 (Figure 5a), while terazosin establishes a series of contacts with Ser residues,

including Ser158, Ser188, and Ser192. For the structurally similar antagonist prazosin, no interactions were observed with receptor conformation α_{1A} [Dox]. Finally, for the antagonist alfuzosin, contacts occur with Glu180 of EC-II and the furan ring and for Ser188 of TM-V with the methylene linker. When the selective antagonist tamsulosin is redocked in receptor conformation α_{1A} [Tam], interactions between the protonated phenethylamine moiety and Glu180 and contacts between the sulfonamide and Asp106 and Ile178 are observed (Figure 5b).

There were poor interactions observed for all the 2-iminoimidazolidinium derivatives 1–4 with receptor conformation α_{1A} -[6]. For the remaining compounds, 6–8, both guanidinium ends of the molecule were involved in forming a number of contacts with the receptor. These generally involve ionic interactions with three out of Asp106, Ile178, Glu180, or Met292 at one guanidinium end, and contacts with a selection of Cys110, Thr111, Ser188, Ser192, or Trp285 at the other end (Figure 5c). Notably, for all the bis-guanidinium compounds, it is the outer two NH_2 groups that interact, and for the majority, both ends of the antagonist participate. To further investigate the differing behavior of the bis-iminoimidazolidinium derivatives with respect to the guanidinium ones, compound 6 was mutated to compounds 1–5, 7, and 8, and further MD simulations (500 ps) were performed. Again, for compounds 1–4 no favorable interactions occur with the receptor, while similar interactions occurred with the bis-guanidinium compounds as in the previous redocked analysis. This finding is consistent with our experimentally determined activities, which indicated a higher activity for the guanidinium compounds compared to the imidazolidinium ones.⁸

Examination of Interactions of Antagonists 9–17 with the Ligand-Induced α_{1A} -ARs. The receptor conformations were used for docking a series of known selective (α_{1A} -AR) and nonselective (α_1 -AR) antagonists 9–17, none of which were initially involved in the production of the ligand-induced α_{1A} -AR conformations. Hence, this study is a form of ligand screening for which a myriad of ligand/receptor interactions emerged. The following analysis focuses on those antagonists

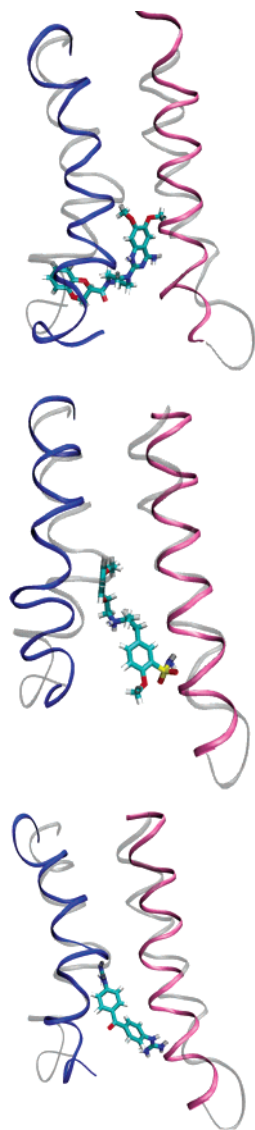


Figure 4. The original uncomplexed conformation (final I) is in gray, while after 1 ns TM-III is in mauve and TM-V is in blue. TM-III and TM-V were superimposed using the fitting protocol of Swissprot. The α_{1A} -Dox complex (upper), α_{1A} -Tam complex (middle), and the α_{1A} -6 complex (lower) are indicated.

that are stably anchored with Asp106 in the postulated binding site of the three receptor conformations over the 500-ps simulations.

For receptor conformation α_{1A} [Dox], interactions occurred with Asp106 for antagonists **10** and **14**, which are thought to be selective α_{1A} -AR antagonists. In complex α_{1A} [Dox]-**10**, a contact between Asp106 and the ether oxygen is formed, while the piperazine moiety interacts with Ile178, Glu180, and Ser188. In the case of complex α_{1A} [Dox]-**14**, the protonated nitrogen of **14** forms ionic interactions with Asp106 and Met292, while Glu180 contacts with a methylene group neighboring the amino group.

For the α_{1A} [Tam] receptor conformation, interactions with Asp106 occur with antagonists **14** and **16** (which are selective α_{1A} -AR antagonists). For the α_{1A} [Tam]-**14** complex, Asp106 forms a contact with an oxygen of the dioxane ring, while Glu180 interacts with the methoxy group. In the case of α_{1A} [Tam]-**16**, a methylene group of **16** interacts with Asp106, Glu180, and Ser188, while Ile178 interacts with the dimethoxy phenyl ring.

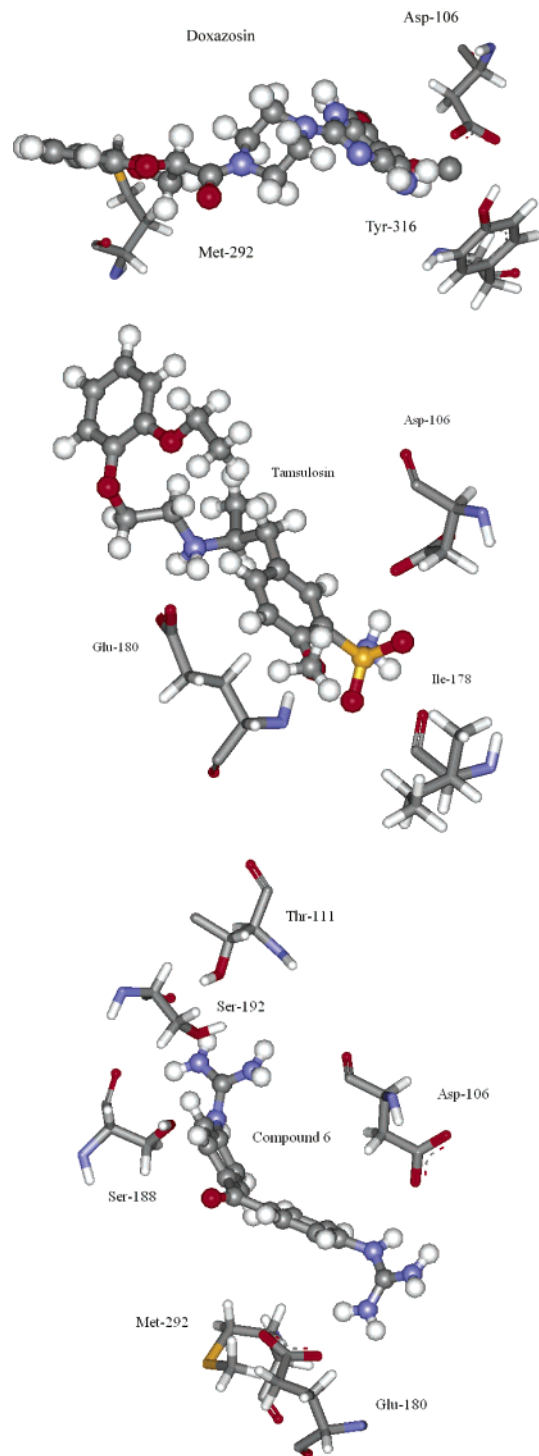


Figure 5. Binding modes of (a) doxazosin in the α_{1A} -Dox receptor conformation, (b) tamsulosin in the α_{1A} -Tam receptor conformation, and (c) compound **6** in the α_{1A} -6 receptor conformation.

For the α_{1A} [6] receptor, interactions occurred with Asp106 for compounds **10–12** and **15–16**. Compound **10** interacts with Asp106 through the methyl group (on the pyrimidinedione ring). Compound **11** contacts with Asp106 and Glu180 through two carbons of the piperazine ring. Compound **12** forms ionic interactions through the protonated nitrogen with Asp106 and Glu180 and through a piperazine nitrogen with Ser188. Compound **15** has an interaction between the protonated nitrogen and Asp106, while a secondary interaction occurred between the methyl linker and Asp106. Finally, compound **16** interacts

with Asp106 through a methoxy group and with Glu180 through a methylene linker.

Conformational Flexibility of Ligands 9–17 in the Ligand-Induced α_{1A} -ARs. The conformational dynamics of the ligands are an important consideration in understanding the various receptor conformations and how they affect binding. The time-dependent variation of the flexible torsions for ligands 9–17 in the three ligand-induced receptor structures was examined over the course of the MD simulations. Most of the ligand conformations are quite rigid across the MD simulations, as many of the ligands have quite restricted degrees of freedom. Compounds 10–15 and 17 show almost fixed torsional angles except in a specific degree of freedom. For compound 10, larger conformational flexibility was observed for the torsion into the trifluoro group across the receptor conformations. For compound 12, torsional flexibility was observed at the ethoxy group, while for compounds, 13–15 torsional flexibility occurred at the methoxy groups. Finally, for compound 17, torsional flexibility was observed across the linker region.

Despite the rigid conformations of the ligands across the individual MD simulations, their conformations are quite different, resulting in very different final binding modes and indicating the significant influence of the initial receptor conformation. For example, the three final binding modes of compound 11 with the antagonist-induced receptor conformations are shown in Figure 6. In the α_{1A} [Dox] receptor conformation, compound 11 is quite extended, while in the α_{1A} [Tam] receptor conformation, this is not possible as the binding site is quite closed. Finally, for the α_{1A} [6] receptor conformation, the ligand is enclosed in the binding site. As a consequence of the different binding modes, across the antagonist-induced receptor conformations the final ligand torsional differences all vary markedly from the uncomplexed conformation and from each other (see Table 3).

Although most of the ligands are quite rigid across the MD simulations, the exceptions are compounds 9 and 16. For compound 9, variations in the flexible linker torsion into the piperazine were observed particularly between 180 and 280 ps in the α_{1A} [Dox] conformation. Compound 9 is notably extended in the final binding mode with the α_{1A} [Dox] conformation (see Figure 7), and this torsion is 178.1° in the final conformation compared with 65.8° in the uncomplexed conformation. This linker torsion coupled with the bond between the linker N and the neighboring C (torsion 2 in the scheme of Table 3) in the α_{1A} [Tam] conformation also varies considerably across the simulation, while no variation was observed in the torsional angles of the ligand for the α_{1A} [6] simulation. The specific torsions of the final binding modes are given in Table 3 coupled with the illustration of the uniqueness of the conformations of compound 9 in the various receptor conformations in Figure 7.

For compound 16, a conformational change occurred at the fused ring (torsion 1 in the diagram of Table 3) at 180 ps in the α_{1A} [Dox] conformation, a conformational change after 250 ps at this linker and at the methoxy group occurred with the α_{1A} -[Tam] conformation, and all torsions were found to conformationally change between 200 and 400 ps with the α_{1A} [6] conformation (see Table 3). Again, an extended ligand conformation is observed with the α_{1A} [Dox] conformation, while different orientations were observed for the α_{1A} [Dox] and α_{1A} -[6] receptor conformations (see Figure 8). Hence, for compounds 9 and 16, differences in ligand conformation are observed for the three ligand-induced receptor conformers as the ligand adapts to the subtle differences in each binding site.

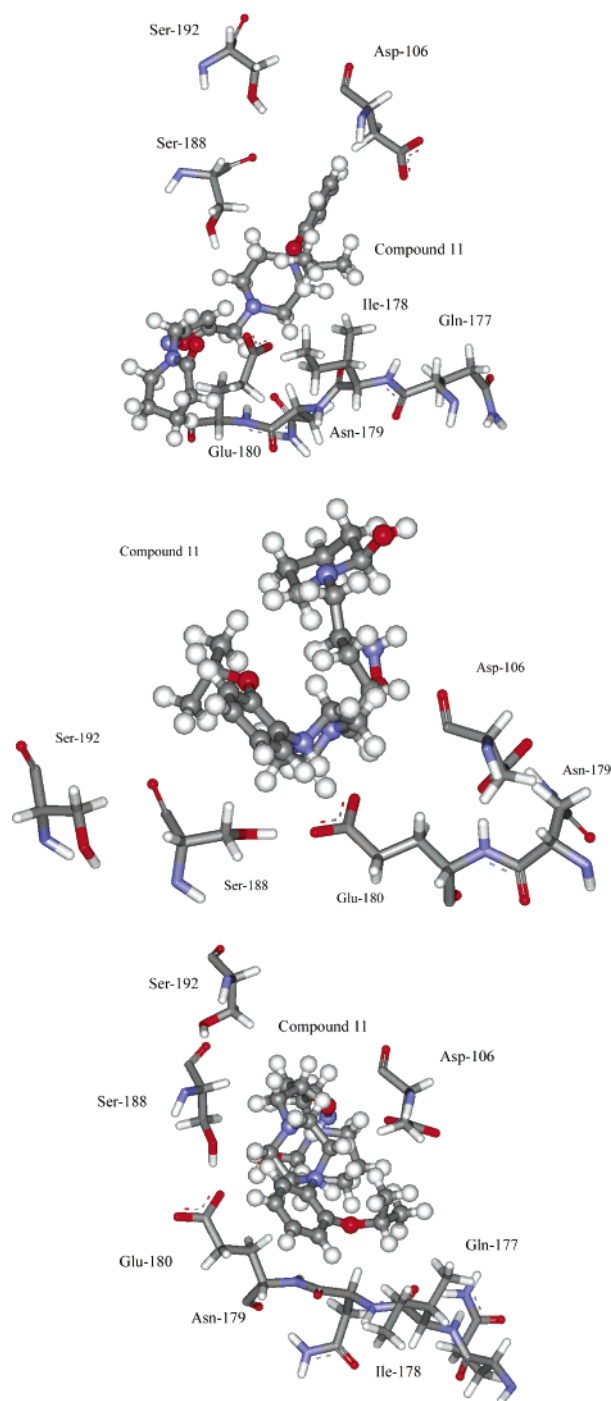
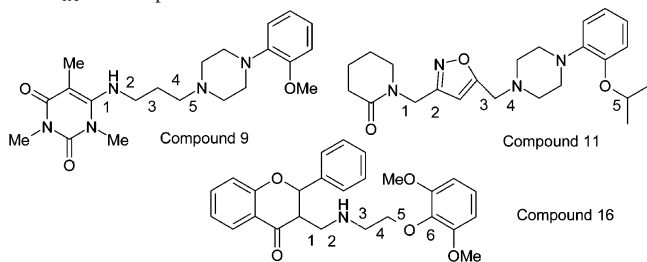


Figure 6. Compound 11 bound in the α_{1A} -Dox (upper), α_{1A} -Tam (middle), and α_{1A} -6 (lower) receptor conformation.

Examination of Binding Affinities for Antagonists 9–17 with the Ligand-Induced α_{1A} -ARs. To compare the relative binding affinities (BAs) of the screened ligands (9–17) for the different receptor conformations we have determined the BAs utilizing the empirical scoring function Xscore.²⁶ The predicted antagonist affinities range from 4.66 to 7.20, with all but one (compound 13 in receptor α_{1A} [6]) in a region that can be assigned to medium-affinity drugs ($5.0 < -\log K_d < 8.0$).²⁷ In Table 4, the complexes are shown in order of decreasing affinity, with the best ranks assigned to complexes with the highest BA. First, it should be noted that the complex with the highest BA varied over the three receptor conformations, ranging from compound 9 for α_{1A} [Dox], compound 12 for receptor conformation α_{1A} [Tam], and compound 11 for receptor conformation α_{1A} -

Table 3. Comparison of the Final Values for the Flexible Torsions of Compounds **9**, **11**, and **16** Complexed with the α_{1A} -Dox, α_{1A} -Tam, and α_{1A} -6 Receptor Conformations


| compd | receptor | torsional angles (deg) | | | | | |
|-----------|---------------------|------------------------|--------|--------|--------|--------|--------|
| | | 1 | 2 | 3 | 4 | 5 | 6 |
| 9 | uncomplexed | 77.8 | 154.8 | -169.6 | 20.7 | 65.8 | - |
| 9 | α_{1A} [Dox] | 63.7 | 126.5 | -174.2 | 62.4 | 178.1 | - |
| 9 | α_{1A} [Tam] | 146.3 | 123.7 | 72.3 | -113.1 | -53.5 | - |
| 9 | α_{1A} [6] | 104.3 | -155.1 | 57.4 | 173.0 | -74.9 | - |
| 11 | uncomplexed | 84.2 | -82.8 | 112.2 | 81.2 | -62.2 | - |
| 11 | α_{1A} [Dox] | -62.5 | 63.0 | 156.3 | 152.4 | 115.9 | - |
| 11 | α_{1A} [Tam] | 46.6 | 61.1 | -163.3 | 173.6 | 174.9 | - |
| 11 | α_{1A} [6] | -63.6 | -12.1 | 5.4 | 85.4 | -149.2 | - |
| 16 | uncomplexed | 55.3 | -177.0 | -61.0 | -39.1 | -86.9 | -71.7 |
| 16 | α_{1A} [Dox] | 68.5 | 165.6 | -62.3 | -46.5 | 171.2 | -110.2 |
| 16 | α_{1A} [Tam] | 47.0 | -156.6 | 84.0 | -105.7 | -174.9 | 108.0 |
| 16 | α_{1A} [6] | 155.9 | -102.6 | 68.7 | 49.9 | 177.0 | 48.0 |

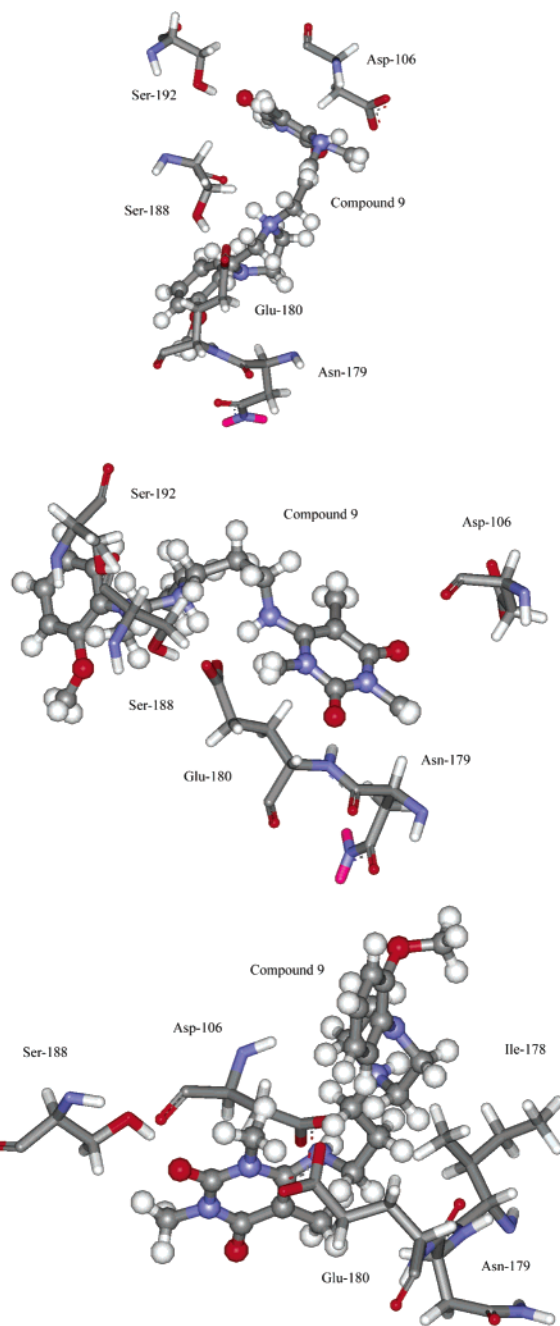
[6]. Furthermore, the remaining antagonists are ranked differently for the three induced receptor conformations. This discrepancy may be a consequence of not inducing an appropriate receptor conformation for that class of ligand. This is consistent with our postulate that it is necessary to induce a receptor conformation for each structural class being studied. Further factors in the observed discrepancies may be related to the quality of the available scoring functions and that our dataset may not be large enough to be able to distinguish clearly between ligands of high and low affinity.

Discussion and Conclusions

In this study, we used a number of antagonists to develop ligand-induced receptor conformations of the α_{1A} -AR through MD simulations allowing for receptor flexibility and optimization of the binding pocket. Compared to the uncomplexed receptor, different conformations emerged for TM-V, with the ligand-induced receptor conformations α_{1A} [Dox] and α_{1A} [6] having a marked effect at Pro196, while for conformation α_{1A} -[Tam], the helix has straightened relative to the uncomplexed form. This movement allows for a change in the interactions of the antagonists with the α_{1A} -AR.

Through our refinement protocol, we have succeeded in obtaining binding models that are qualitatively consistent with the available mutagenesis data for α_1 -AR antagonists. In terms of the ionic interactions of our developed antagonists, the bis-imidazolium compounds did not interact as strongly as the guanidinium compounds with any receptor model. For compounds **5**–**8**, interactions of both bis-guanidinium moieties with different residues of the active site were observed.

Furthermore, our receptor models were used to test binding of a range of known α_1 -AR antagonists. For the screening of the antagonists **9**–**17**, a number of ionic interactions involved the EC-II residues Ile178, Asn179, and Glu180 and also residue Ser188 in TM-V, which were consistent with the available body of experimental work. However, our binding site analysis also indicates that receptor conformations induced by the interaction with one class of antagonist are not directly suitable for screening of another structural class. It appears necessary

**Figure 7.** Compound **9** bound in the α_{1A} -Dox (upper), α_{1A} -Tam (middle), and α_{1A} -6 (lower) receptor conformation.

to produce an “antagonist-bound” receptor form for each class or family of antagonist to evaluate their detailed interactions with the α_{1A} -AR and establish possible binding modes.

The work of Evers et al.²⁰ concluded that rhodopsin-based homology models may be used as the structural basis for GPCR lead finding and compound optimization. Such studies can provide valuable information for antagonist binding sites; however, our study would indicate that this approach will favor antagonists of a similar conformation to that used in developing the homology model. Indeed, those antagonists identified by Evers et al.²⁰ using virtual screening have similar chemical conformations to the antagonist used in developing their receptor model.

To obtain novel antagonists, a greater degree of flexibility within the receptor model will be required. This could be achieved through the use of multiple ligand conformations obtained for related classes either through a dynamic approach,

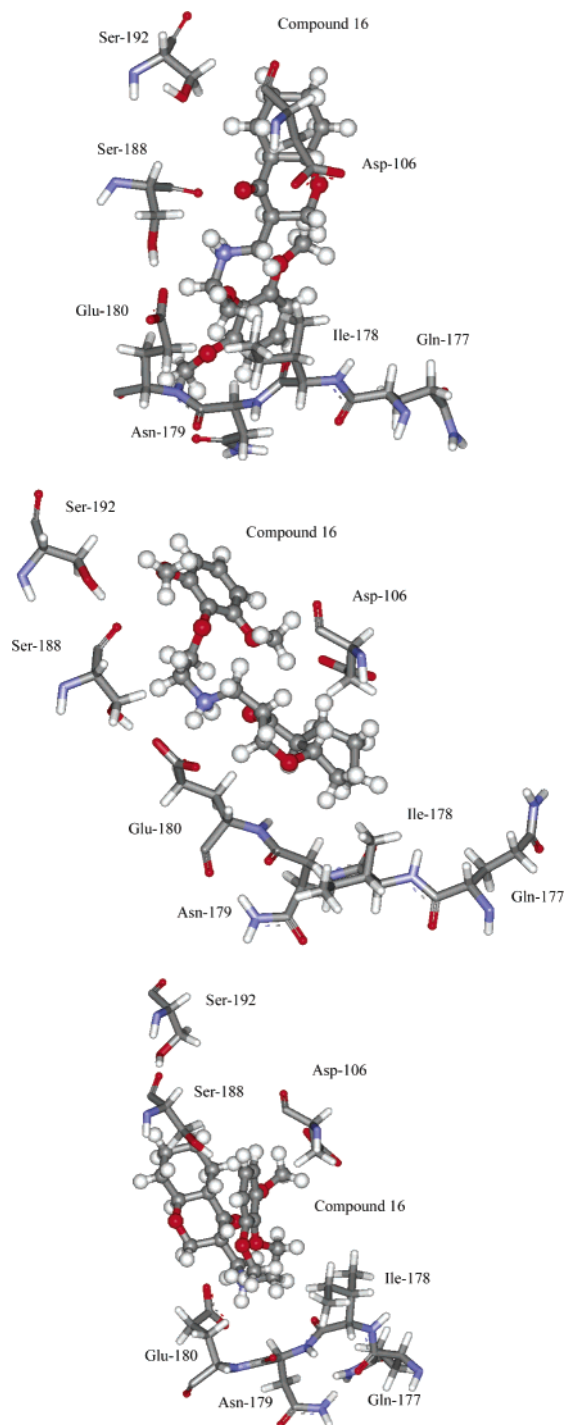


Figure 8. Compound **16** bound in the α_{1A} -Dox (upper), α_{1A} -Tam (middle), and α_{1A} -**6** (lower) receptor conformation.

as used here, or possibly through homology modeling utilizing ligand restraints.²⁰ The advantage of our approach is that the binding site and conformational changes occur as part of the iterative cycle of docking and dynamics, allowing new interactions to form and small but possibly vital conformational changes to occur as the ligand is accommodated in the binding site. Such a procedure is a more rational approach than direct docking into a rigid rhodopsin-based homology model, as it allows for increased flexibility of the receptor. Our approach can, in principle, be applied to any member of the GPCR family with known ligand information and site-directed mutagenesis data. The predicted 3D conformations and antagonist binding modes could also be used in designing mutagenesis experiments

Table 4. Ranking of Antagonists (**9**–**17**) for the Various Receptor Conformations, According to the Binding Affinities Determined Using the Xscore Scoring Function^a

| rank | ranking of compounds by binding affinity (compd no.) | | |
|------|--|---------------------|----------------------------|
| | α_{1A} [Dox] | α_{1A} [Tam] | α_{1A} [6] |
| 1st | 6.99 (9) | 6.75 (12) | 7.25 (11) |
| 2nd | 6.95 (15) | 6.55 (17) | 7.20 (17) |
| 3rd | 6.79 (11) | 6.30 (16) | 6.59 (15) |
| 4th | 6.86 (12) | 6.23 (11) | 6.39 (12) |
| 5th | 6.27 (16) | 6.14 (13) | 6.35 (10) |
| 6th | 6.24 (10) | 6.07 (10) | 6.22 (9) |
| 7th | 6.14 (17) | 5.97 (9) | 6.05 (16) |
| 8th | 5.88 (14) | 5.59 (14) | 4.87 (14) |
| 9th | 5.52 (13) | 5.59 (15) | 4.66 (13) |

^a Compounds are ranked in order of decreasing affinity of the ligand for the receptor.

to validate the conformation of the binding sites of the computational models.

Experimental Methods

We have studied the conformational changes that occurred upon antagonist binding using a ligand-induced receptor conformation approach. This involved the following:

(1) Three antagonists, doxazosin, tamsulosin, and compound **6**, were docked with our previously developed homology model of the α_{1A} -AR¹⁸ to examine their initial interactions.

(2) Molecular dynamics simulations (1 ns) of the docked complexes were performed in a H₂O/CHCl₃/H₂O membrane mimic to simulate structural changes to the α_{1A} -AR upon antagonist binding within a membrane environment.

(3) A series of 22 known antagonists were docked into the three “antagonist-bound” receptor forms developed in step 2.

(4) Further MD simulations (500 ps) were performed on the antagonist/receptor complexes to determine the interacting residues and the various binding modes adopted by the ligands in the three “antagonist-bound” receptor conformations.

Preparation of the α_{1A} -AR and Ligands. The initial α_{1A} -AR conformation was obtained from our earlier study of α_{1A} -AR homology models.¹⁸ The three antagonists, doxazosin, tamsulosin, and compound **6**, were chosen to produce three ligand-induced α_{1A} -AR conformations. Doxazosin was selected as an example of an α_1 -AR subtype-nonselective antagonist and tamsulosin as a selective α_{1A} -AR antagonist, both of which are currently available on the market. Finally, compound **6** was chosen as it exhibited the best activity at the α_{1A} -AR of our developed compounds. The nitrogens with the highest determined proton affinity (PA) in our previous study were protonated for each antagonist and optimized.²⁸ Atomic point charges for the antagonists were obtained from a fit to the electrostatic potential calculated during density functional theory (DFT) structural optimizations using the B3LYP hybrid functional and the 6-31G* basis set in Gaussian 98.²⁹

Ligand Docking. To date, most mutagenesis studies have focused on the molecular interactions of the catecholamine agonists adrenaline (AD) and noradrenaline (ND), with different adrenoceptor subtypes.³⁰ Mutagenesis studies of the α_2A -AR and β_2 -ARs suggest that the amino group of the endogenous catecholamines forms an electrostatic interaction with the carboxylate side chain of an Asp residue in TM-III (Asp106 in α_{1A} -AR), which is highly conserved in all aminergic GPCRs. Additionally, Ser residues in TM-V may interact with the catechol hydroxyl groups.^{31,32} Such interactions using a ligand-induced receptor conformation approach have been theoretically examined in our previous work.³³ Furthermore, Zhao et al.³⁴ determined that residues of the second extracellular loop (EC-II), including Gln177, Ile178, and Asn179, may be responsible for selective antagonist binding for the α_{1A} -AR over the α_{1B} -AR. The defined antagonist binding site included those residues important in the mutagenesis studies and was taken as all residues within 10 Å of Asp106 in TM-III, Ser188 and Ser192 in TM-V, and residues 177–179 in EC-II. The initial complexes

were obtained using Dock 4.0³⁵ and were optimized using the FlexiDock³⁶ routine of Sybyl 6.9, to allow some flexibility to selected receptor residues.

Molecular Dynamics Simulations. The employed MD protocol using the Amber 7.0 suite³⁷ was similar to that used previously¹⁸ and will be briefly described here. The simulation cell was heated to 300 K over 5 ps with equilibration performed using backbone restraints for 5 ps at each of 15, 10, and 5 kcal mol⁻¹ followed by 65 ps without restraints. Periodic boundary conditions were applied in all three dimensions with the Particle Mesh Ewald (PME) method being used to treat the long-range electrostatic interaction. Non-bonded interactions were calculated for 1–4 interactions and higher using a cutoff radius of 9 Å. Further analyses were performed using Amber 7.0 and the Gromacs (v 3.1.4) tools.³⁸ Hydrogen bonds (HBs) were defined geometrically, with the donor–acceptor hydrogen angle having to be less than 60° and the donor–acceptor distance ($d[\text{donor}\cdots\text{acceptor}]$) being less than 4 Å. Amber was also used to optimize the docked and final dynamical conformers using steepest descent (250 steps) and conjugate gradient (750 steps) energy minimization methods.

The study of Wymore et al.³⁹ concluded that the same qualitative features were achieved in comparative simulations of the biphasic (hexane/H₂O) and micellar (SDS, dodecyl sulfate) system to that of the phospholipid dimyristoylphosphatidyl (DMPC). In this work, to facilitate routine simulations of molecules in membrane-like surroundings, the behavior of the antagonist/receptor complexes in a membrane mimic (H₂O/CHCl₃/H₂O) are examined. The CHCl₃ and H₂O phases represent the fatty acid chain matrix and the neighboring polar phase, respectively, and allow the systems to sample more conformational space within the simulation time available than a computationally expensive full lipid model, while maintaining an all atom approach. Counterions (Cl⁻) were added to ensure a charge neutral cell, by replacing solvent molecules at sites of high electrostatic potential.

For the antagonists, the molecular mechanical atom types and parameters were obtained from the general Amber force field (GAFF).⁴⁰ Some additional parameters concerned with the guanidinium portion of compounds **1–8** were obtained by analogy to others available in GAFF. These parameters were optimized to best reproduce the theoretical frequencies obtained from DFT calculations (B3LYP/6-31G* level scaled by a factor of 0.9614).⁴¹ These include c2–n2 (420.9 kcal mol⁻¹, 1.38 Å), c2–n2–hn (44.9 kcal mol⁻¹, 120.0°), and h2–c2–n2 (46.1 kcal mol⁻¹, 120.0°). To ensure the suitability of all ligand parameters, short MD simulations of 200 ps were performed for each antagonist in a water box. All subsequent average conformers were examined and determined to be structurally stable.

Acknowledgment. The authors would like to acknowledge the HEA for a PRTL I (Cycle III) grant, TCD for a Trinity College Dublin postgraduate scholarship (G.K.) and Enterprise Ireland for a postgraduate research scholarship (G.K.). The authors would also like to thank Dr. Peter Oliver at RAL for assistance with Mott2 and EPSRC for funding.

References

- Hansson, T.; Oostenbrink, C.; van Gunsteren, W. Molecular Dynamics Simulations. *Curr. Opin. Struct. Biol.* **2002**, *12*, 2, 190–196.
- Matyus, P.; Horvath, K. Alpha-adrenergic approach in the medical management of benign prostatic hyperplasia. *Med. Res. Rev.* **1997**, *17*, 523–535.
- Kirby, R.; McConnell, J. D.; FitzPatrick J. M.; Roehrborn, C.; Boyle, P. (Eds.) *Textbook of Benign Prostatic Hyperplasia*, Isis Medical Media Ltd.: Oxford, UK, 1996.
- Narayan P.; Tewari, A. Overview of alpha blocker therapy of BPH. *Urology* **1998**, *51* (Supplement 4A), April, 38–45.
- Bremner, J. B.; Coban, B.; Griffith, R.; Groenewoud, K. M.; Yates, B. F. Ligand Design for α_1 Adrenoceptor Subtype Selective Antagonists. *Bioorgan. Med. Chem.* **2000**, *8*, 201–214.
- Beduschi, M. C.; Beduschi, R.; Oesterling, J. E. Alpha-blockade therapy for benign prostatic hyperplasia: From a nonselective to a more selective α_{1A} -adrenergic antagonist. *Urology* **1998**, *51*, 861–872.
- Dardonville, C.; Goya, P.; Rozas, I.; Alasua, A.; Martin, I.; Borrego, J. New aromatic iminoimidazolidine derivatives as α_1 -adrenoceptor antagonists: A novel synthetic approach and pharmacological activity. *Bioorg. Med. Chem.* **2000**, *8*, 1567–1577.
- Dannert, M. T.; Alasua, A.; Borrego, M. J.; Dardonville, C.; Sanchez, M.; Martin, M. I. XXIV Congreso de la Sociedad Española de Farmacología. *Methods Findings Exp. Clin. Pharmacol.* **2002**, *24*, 158.
- Gross, G.; Hanft, G.; Rugevics, C. 5-methyl-urapidil discriminates between subtypes of the α_1 -adrenoceptor. *Eur. J. Pharmacol.* **1988**, *151*, 333–335.
- Blue, D. R.; Ford, A. P. D. W.; Morgans, D. J.; Padilla, F.; Clarke, D. E. Preclinical pharmacology of a novel $\alpha_1A/1L$ adrenoceptor antagonist. *NeuroUrol. Urodyn.* **1996**, *14*, 345.
- Kuo, G.; Prouty, C.; Murray, W. V.; Pulito, V.; Jolliffe, L.; Cheung, P.; Varga, S.; Evangelisto, M.; Wang, J. Design, synthesis and conformation-activity relationships of phthalamide-phenylpiperazines: A novel series of potent and selective alpha (1a) adrenergic receptor antagonists. *J. Med. Chem.* **2000**, *43*, 2183–2195.
- Barbaro, R.; Betti, L.; Botta, M.; Corelli, F.; Giannaccini, G.; Maccari, L.; Manetti, F.; Strappaghetti, G.; Corsano, S. Synthesis and biological activity of new 1,4-benzodioxan-arylpiperazine derivatives. Further validation of a pharmacophore model for alpha1-adrenoceptor antagonists. *Bioorg. Med. Chem.* **2002**, *10*, 361–369.
- Chern, J. W.; Tao, P.; Wang, K.; Gutcait, A.; Liu, S.; Yen, M.; Chien, S.; Rong, J. Studies on quinazolines and 1,2,4-benzothiadiazine 1,1-dioxides. Synthesis and pharmacological evaluation of tricyclic fused quinazolines and 1,2,4-benzothiadiazine. *J. Med. Chem.* **1998**, *41*, 3128–3141.
- Quaglia, W.; Pignini, M.; Piergentili, A.; Giannella, M.; Gentili, F.; Marucci, G.; Carrieri, A.; Carotti, A.; Poggesi, E.; Leocardi, A.; Melchiorre, C. Conformation activity relationships in 1,4-benzodioxan-related compounds. Selectivity of 4-phenylchroman analogues for alpha(1) adrenoceptor subtypes. *J. Med. Chem.* **2002**, *45*, 1633–1643.
- (a) Kava, M. S.; Blue Jr, D. R.; Vimont, R. L.; Clarke, D. E.; Ford, A. P. α_1L -adrenoceptor mediation for lower urinary tract tissues of man. *Br. J. Pharmacol.* **1998**, *123*, 1359–1366. (b) Williams, T. J.; Blue, D. R.; Daniels, D. V.; Davis, B.; Elworthy, T.; Gever, J. R.; Kava, M. S.; Morgans, D.; Padilla, F.; Tassa, S.; Vimont, R. L.; Chapple, C. R.; Chess-Williams, R.; Eglen, R. M.; Clarke, D. E.; Ford, A. P. D. W. In vitro α_1 -adrenoceptor pharmacology of Ro 70-0004 and RS-100329, novel α_1A -adrenoceptor selective antagonists. *Br. J. Pharmacol.* **1999**, *127*, 252–258.
- Palczewski, K.; Kumasaka, T.; Hori, T.; Behnke, C. A.; Motohima, H.; Fox, B. A.; Trong, I. L.; Teller, D. C.; Okada, T.; Stenkamp, R. E.; Yamamoto, M.; Miyano, M. Crystal conformation of rhodopsin: A G protein-coupled receptor. *Science* **2000**, *289*, 739–745.
- Okada, T.; Fujiyoshi, Y.; Silow, M.; Navarro, J.; Landau, E. M.; Shichida, Y.; Functional role of internal water molecules in rhodopsin revealed by X-ray crystallography. *PNAS* **2002**, *99* 5982–5987.
- Kinsella, G. K.; Rozas, I.; Watson, G. W. Computational study of the α_1A adrenoceptor, *Biochem. Biophys. Res. Commun.* **2004**, *324*, 916–921.
- Bissantz, C.; Bernard, P.; Hibert, M.; Rognan, D. Protein-based virtual screening of chemical databases. II. Are homology models of G-protein coupled receptors suitable targets? *Proteins* **2003**, *50*, 5–25.
- Evers, A.; Klabunde, T. Conformation-based drug discovery using GPCR homology modelling: Successful virtual screening for antagonists of the alpha1A adrenergic receptor. *J. Med. Chem.* **2005**, *48*, 1088–1097.
- Pedretti, A.; Silva, M. E.; Villa, L.; Vistoli, G. Binding site analysis of full length alpha-1A adrenergic receptor using homology modeling and molecular docking. *Biochem. Biophys. Res. Commun.* **2004**, *319*, 493–500.
- Visiers, I.; Ballesteros, J. A.; Weinstein, H. Three-dimensional representations of G protein-coupled receptor structures and mechanisms. *Methods Enzymol.* **2002**, *343*, 329.
- Ballesteros, J.; Palczewski, K. G protein-coupled receptor drug discovery: Implications from the crystal structure of rhodopsin. *Curr. Opin. Drug Discov. Devel.* **2001**, *4*, 561.
- Sansom, S.P.; Weinstein, H. Hinges, swivels and switches: The role of prolines in signalling via transmembrane alpha-helices. *Trends Pharmacol. Sci.* **2000**, *21*, 445.
- von Heijne, G. Proline-kinks in Transmembrane a-helices. *J. Mol. Biol.* **1991**, *218*, 499.

- (26) Wang, R.; Lai, L.; Wang, S. Further development and validation of empirical scoring functions for conformation-based binding affinity prediction. *J. Comput. Aided Mol. Des.* **2002**, *16*, 11–26.
- (27) Wang, R.; Lu, Y.; Fang, X.; Wang, S. An extensive test of 14 scoring functions using PDBbind refined set of 800 protein–ligand complexes. *J. Chem. Inf. Comput. Sci.* **2004**, *44*, 2114–2125.
- (28) Kinsella, G. K.; Rozas, I.; Watson, G. W. Theoretical proton affinities of $\alpha 1$ adrenoceptor ligands. *Bioorg. Med. Chem.* **2005**, in press.
- (29) Frisch, M. J.; Trucks, G. W.; Schlegel, H. B.; Scuseria, G. E.; Robb, M. A.; Cheeseman, J. R.; Zakrzewski, V. G.; Montgomery, J. A., Jr.; Stratmann, R. E.; Burant, J. C.; Dapprich, S.; Millam, J. M.; Daniels, A. D.; Kudin, K. N.; Strain, M. C.; Farkas, O.; Tomasi, J.; Barone, V.; Cossi, M.; Cammi, R.; Mennucci, B.; Pomelli, C.; Adamo, C.; Clifford, S.; Ochterski, J.; Petersson, G. A.; Ayala, P. Y.; Cui, Q.; Morokuma, K.; Salvador, P.; Dannenberg, J. J.; Malick, D. K.; Rabuck, A. D.; Raghavachari, K.; Foresman, J. B.; Cioslowski, J.; Ortiz, J. V.; Baboul, A. G.; Stefanov, B. B.; Liu, G.; Liashenko, A.; Piskorz, P.; Komaromi, I.; Gomperts, R.; Martin, R. L.; Fox, D. J.; Keith, T.; Al-Laham, M. A.; Peng, C. Y.; Nanayakkara, A.; Challacombe, M.; Gill, P. M. W.; Johnson, B.; Chen, W.; Wong, M. W.; Andres, J. L.; Gonzalez, C.; Head-Gordon, M.; Replogle, E. S.; Pople, J. A. *Gaussian 98* (Rev A.11); Gaussian, Inc., Pittsburgh, PA, 2001.
- (30) Hamaguchi, N.; True, T.; Saussy, D. L.; Jeffs, P. W. Phenylalanine in the second membrane-spanning domain of alpha 1A-adrenergic receptor determines subtype selectivity of dihydropyridine antagonists. *Biochemistry* **1996**, *35*, 14312–14317.
- (31) Cavalli, A.; Fanelli, F.; Taddei, C.; de Benedetti, P. G.; Cotechia, S. Amino acids of the $\alpha 1B$ -adrenergic receptor involved in agonist binding: Differences in docking of catecholamines to receptor subtypes. *FEBS Lett.* **1996**, *399*, 9–13.
- (32) Piascik, M. T.; Perez, D. M. Alpha 1-adrenergic receptors: New insights and directions. *J. Pharmacol. Exp. Ther.* **2001**, *298*, 403–410.
- (33) Kinsella, G. K.; Rozas, I.; Watson, G. W. Modelling the interaction of catecholamines with the $\alpha 1A$ adrenoceptor—Towards a ligand-induced receptor conformation. *J. Comput. Aided Mol. Des.* **2005**, *19*, 357–367.
- (34) Zhao, M.; Hwa, J.; Perez, D. M. Identification of critical extracellular loop residues involved in alpha 1-adrenergic receptor subtype-selective antagonist binding. *Mol. Pharmacol.* **1996**, *50*, 1118–1126.
- (35) Kuntz, I. D. Conformation-based strategies for drug design and discovery. *Science* **1992**, *257*, 1078–1082.
- (36) *Sybyl 6.9, Molecular Modelling System*; Tripos Associates: St. Louis, MO.
- (37) Case, D. A.; Pearlman, D. A.; Caldwell, J. W.; Cheatham, T. E., III; Wang, J.; Ross, W. S.; Simmerling, C. L.; Darden, T. A.; Merz, K. M.; Stanton, R. V.; Cheng, A. L.; Vincent, J. J.; Crowley, M.; Tsui, V.; Gohlke, H.; Radmer, R. J.; Duan, Y.; Pitner, J.; Massova, I.; Seibel, G. L.; Singh, U. C.; Weiner, P. K.; Kollman, P. A. *Amber 7*; University of California, San Francisco, 2002.
- (38) Berendsen, H. J. C.; Postma, J. P. M.; van Gunsteren, W. F.; DiNola, A.; Haak, J. R. Molecular Dynamics with coupling to an external bath. *J. Chem. Phys.* **1984**, *81*, 3684–3690.
- (39) Wymore, T.; Wong, T. C. 45th Annual Meeting of the Biophysical Society, Boston, MA, 2001.
- (40) Wang, J.; Wolf, R. M.; Caldwell, J. W.; Kollman, P. A.; Case, D. A. Development and testing of a general Amber force field. *J. Comput. Chem.* **2004**, *25*, 1157–1174.
- (41) Scott, A. P.; Radom, L. Harmonic vibrational frequencies: An evaluation of Hartree–Fock, Møller–Plesset, quadratic configuration interaction, density functional theory and semiempirical scale factors. *J. Phys. Chem.* **1996**, *100*, 16502–16513.

JM0503751